

Terrestrial Laser Scanning Technology for Deformation Monitoring of a Large Suspension Roof Structure

Mill, T. and Ellmann, A.

Tallinn University of Technology, Faculty of Civil Engineering, Dept. of Road Engineering, Chair of Geodesy, Ehitajate tee 5, 19086 Tallinn, Estonia, Web site: <http://www.ttu.ee>
E-mail: tarvo@tktk.ee, Artu.Ellmann@ttu.ee

Abstract

Terrestrial laser scanning (TLS) technology has found extensive use in the construction industry in recent years, as it makes it possible to acquire high resolution data quickly and accurately. The study uses TLS for deformation monitoring of a suspension roof structure of a large acoustic screen (73 m wide, 37 m long, 32 m high) at the Tallinn song festival grounds in Estonia. The structural geometry and behaviour of the acoustic screen was determined under three different load conditions. First, the initial shape of the acoustic screen with no load was measured. The second scanning epoch was carried out when the acoustic screen was covered with 70 t of melting snow. Significant deformations of the structure (reaching -11.3 cm) due to the snow load were detected. The third scan was carried out nearly three months after by which time the acoustic screen was assumed to recover its original shape. Somewhat surprisingly, the structure did not fully recover its pre-winter shape, with residual deformations of up to -3.8 cm. The study highlights the benefits of monitoring complex and inaccessible structures using TLS. The study also calls attention to the importance of monitoring complex structures periodically in order to assess structural changes due to environmental causes – wind and snow loads. Monitoring results allow managers of the structure to take any measures necessary to maintain its structural integrity and safety.

Key words: terrestrial laser scanning, deformation monitoring, suspension roof structure

1 INTRODUCTION

TLS technology has been used widely in civil engineering for at least a decade now. Due to rapid technological development, the metrological characteristics of TLS instruments have improved to such a degree, that TLS is now suitable in applications with accuracies better than 10 mm (e.g. Lichti 2008, Soudarissanane, *et al.* 2011, González-Jorge, *et al.* 2011).

Applications of TLS technology for deformation monitoring have been reported by Tsakiri and Pfeifer 2006, González-Aguilera, *et al.* 2008, Riveiroa, *et al.* 2013. The present study deals with the TLS monitoring of a suspension roof structure of a large acoustic screen at the Tallinn song festival grounds in Estonia. The monitoring process was conducted from points of especially designed geodetic network around the structure. The monitoring measurements were carried out in three time epochs: in November, before the first snowfall and onset of the major cold period, to measure the initial state of the screen; in February, under a load of snow,

TS 5 – Deformation measurement

when extreme displacements were expected; and in May, at the end of the cold period, when the complete recovery of the structure was expected. The accuracy of ± 5 mm in TLS survey was aimed at.

2 THE STRUCTURE

The large-scale acoustic screen was erected in 1959 on the Estonian Song and Dance festival grounds in Tallinn, the capital of Estonia. The acoustic screen was designed as a pre-stressed roof network structure which is a hanging of negative Gaussian curvature. The roof of the screen consists of ribbed wooden panels resting on a freely bended bearing cable network. The pre-stressed cable network is formed inside the contour, consisting of two planar arches (Figure 1). The back arch is made of reinforced concrete, the plane being inclined an angle of 19° to the horizon. The front arch consists of a steel tube, partially filled with concrete and inclined at an angle of 58° to the horizon. Both the back and the front arch have common main supports in the form of massive counter-forts (Figure 1), which develop considerable horizontal reactions to the arch forces. Network cables are made of locked-coil wire ropes 38.5 mm in diameter. The dimensions of the structure are the opening of the screen 73 m in width, height of the screen 32 m and length of the screen 37 m. (Kulbach 2007).

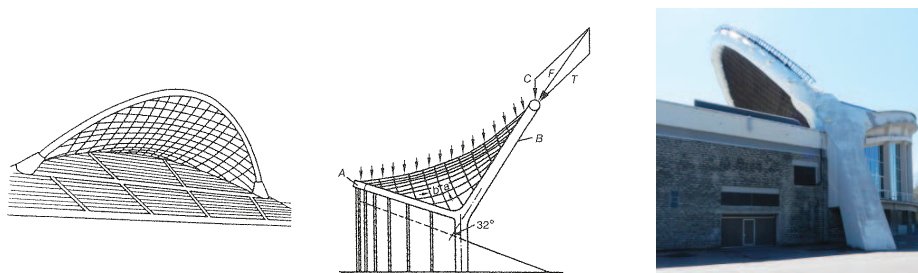


Figure 1 Schemes of the cable network for the acoustic screen (left) and supportive contour arches and a photo of the massive counter-fort (right) of the song festival tribune in Tallinn, the top of the screen reaches 32 m above the ground

3 ESTABLISHMENT OF GEODETIC MONITORING NETWORK

In order to monitor the behaviour of the acoustic screen under different load conditions, a geodetic network with reference points in close proximity to the acoustic screen was established (Figure 2). The locations of the distant points (S2; S3; S4; S8; S9) were selected to be visible from the top of the screen. Planar coordinates (x , y) the points were determined using a total station Trimble M3 (range and angular accuracy ± 2 mm+2 ppm and $5''$, respectively). The traverse was adjusted using Trimble M3 Controller software, applying the Bowditch rule (Schofield and Breach 2007):

$$\delta x_i = \frac{f_{\Delta x}}{\sum_{i=1}^n L_i} L_i \quad (1)$$

$$\delta y_i = \frac{f_{\Delta y}}{\sum_{i=1}^n L_i} L_i \quad (2)$$

where δx_i , δy_i are the coordinate corrections, $f_{\Delta x}$, $f_{\Delta y}$ are the coordinate misclosures, $\sum_{i=1}^n L_i$ is the total length of the traverse, L_i is the (horizontal) length of the i -th traverse leg. The

coordinate misclosures $f_{\Delta x} = -0.001$ m and $f_{\Delta y} = +0.005$ m were achieved, which were further adjusted. The relative error of traverse was achieved to be 1 / 163,419.

The heights (z-coordinate) of the geodetic points were established using an electronic levelling instrument Leica Sprinter 100 (allowing standard deviation height 2.0 mm per 1 km double run) with a standard aluminium staff. The forth and back sights during the levelling were kept equal and two readings were taken from each staff, varying the height of the level. The misclosure of the 0.65 km long levelling loop was -4 mm, which was further adjusted. Thus, the coordinates and heights of the geodetic monitoring network are assumed to be sufficiently accurate for achieving the scope of the research.

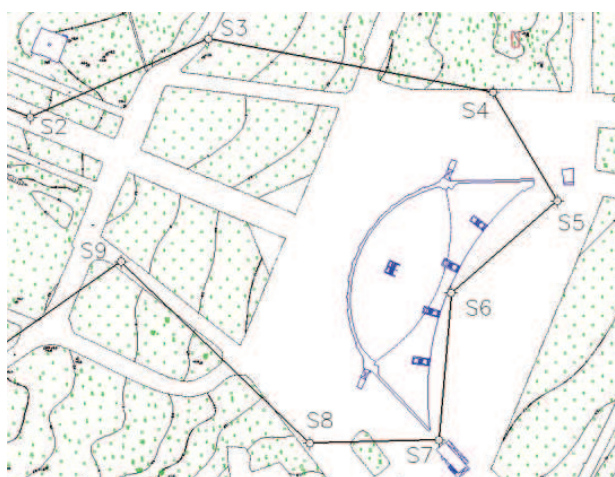


Figure 2 Geodetic monitoring network (reference points S2...S9 embedded in the asphalt pavement), the length of section S5-S6 corresponds to 52.7 m

4 TERRESTRIAL LASER SCANNING TECHNOLOGY

Terrestrial laser scanning describes mainly a ground based static method of high resolution sampling of the entire surface area of the object of interest without direct contact. Thousands of points are collected within seconds. The result of a scan is a large number of points (millions) representing 3D coordinates of the reflecting surface, forming thus a point cloud.

Since the speed of light is known, the measuring of the time delay created by the laser signal travelling from the source to a reflective target surface and back to a signal detector is used to calculate the distance. Such systems are also known as time-of-flight (TOF) and phase shift (PS) technologies.

The TOF method utilises short laser pulses, the distance being determined by the travel time of the signal to the object and back. TOF laser scanners are mainly characterised by a typical data acquisition rate of up to 50,000 points per second and working ranges normally within a few hundred meters.

The PS method utilises signal modulation and applies continuous wave lasers, the distance being determined by the phase shift of the sent and received waveforms. PS laser scanners can be characterised by a very high data acquisition rate of up to 1 million points per second or even more. Normally the working range of PS scanners is limited by the decreasing intensity of the modulated waves, and the range is limited to approximately 100 meters.

4.1 TERRESTRIAL LASER SCANNING OF THE ACOUSTIC SCREEN

For the case study a TOF scanner Leica ScanStation C10 was used. The maximum range of the device is 300 m with a 360 x 270° field of view and a maximum scanning rate of up to

50,000 points/sec. The range and angle accuracy specifications are ± 4 mm and $\pm 12''$ arc-sec, respectively. The scanning was carried out in November 2012, February 2013 and May 2013. Due to the small incidence angles (mainly within 30°) the range measurement precision determines the precision of the resulting precision of the scanned height. Using the equation of error propagation law for non-linear function of random variables

$$\sigma^2(\Delta\hat{z}) = \sum_{i=1}^n \left(\frac{\partial f}{\partial w_i} \right)^2 \cdot \sigma^2(w_i) \quad (3)$$

where $\sigma^2(\Delta\hat{z})$ denotes the combined variance of height increment with respect to the scanner origin, note that $\Delta\hat{z}$ is an estimate (derived from the TLS range and angle measurements) of the actual height increment z , f is the (non-linear) function $z=f(w_i), i=1, \dots, n$, consisting of random observables $(w_i), i=1, \dots, n$, whereas $\sigma^2(w_i)$ is the error of individual observables. The observation equation can be written as

$$\Delta\hat{z}_i = \rho_i \cdot \cos \varphi_i \quad (4)$$

where ρ_i is the i -th slope distance from the scanning station to the reflective surface, φ_i is the i -th zenith angle, z_i is the resulting i -th height increment. Inserting Eq.4 into Eq. 3 and calculating derivatives the combined standard uncertainty $\sigma(\Delta\hat{z})$ of height increment of a survey point is found as

$$\sigma(\Delta\hat{z}) = \sqrt{\cos^2 \varphi_i \cdot \sigma_{dist}^2 + \rho_i^2 \cdot (-\sin \varphi_i)^2 \cdot \sigma_{angle}^2} \quad (5)$$

where σ_{dist} is the scanner's standard distance uncertainty and σ_{angle} is the scanner's standard angular uncertainty. Using the Eq. 5, the numerical value of $\sigma(\Delta\hat{z})$ was calculated as follows

$$\sigma(\Delta\hat{z}) = \sqrt{(\cos 34^\circ 40')^2 \cdot 0.004^2 + 26.4^2 \cdot (-\sin 34^\circ 40')^2 \cdot \left(\frac{12''}{206265''}\right)^2} = \pm 0.0034m$$

Where $34^\circ 40'$ is an average zenith angle (φ) between the zenith of TLS and a direction to a point approximately in the centre of the acoustic screen, 26.4 is an average distance from the scanner to observation points in the centre of the screen, numerical values for σ_{dist} and σ_{angle} were taken from the manufacturer's specifications (see above). As a result $\sigma(\Delta\hat{z})$ equals ± 3.4 mm (one sigma), which by adopting the 95% confidence interval level yields an uncertainty of ± 6.8 mm. Thus the uncertainty of two compared data sets equals $6.8 \cdot \sqrt{2} = \pm 9.6$ mm. A TLS survey like any other geodetic survey is affected by various error sources (e.g., setting-up errors, orientation errors, environmental errors, etc.). The actual accumulated uncertainty in height between two TLS epochs was assessed to be less than ± 15 mm with a two sigma confidence level. Hence, height differences exceeding ± 15 mm between two TLS epochs at a location can be considered as actual deformation.

Transformation of point clouds into a common coordinate system was proceeded using direct georeferencing with respect to the ground reference system

$$\mathbf{x}_e = \mathbf{R}(\mathbf{z})\mathbf{x}_i + \mathbf{x}_{scanner} \quad (6)$$

where \mathbf{x}_e is the vector of coordinates of a point in the external coordinate system, $\mathbf{R}(\mathbf{z})$ is the rotation matrix around the z-axis, \mathbf{x}_i is the vector of coordinates of a point in the point cloud in the scanner coordinate system, $\mathbf{x}_{scanner}$ is the vector of coordinates of the origin of the scanner coordinate system with respect to the ground reference system. (Lichti and Gordon 2004)

4.2 SCANNING EPOCHS

The first scanning epoch took place in November 2012, before the winter cold period and first snowfall. The aim of the first epoch was to measure the initial state of the acoustic screen under its own weight. The scanning was conducted at the front of the screen and from on the top of the screen. The scanning at on the top of the screen was performed to capture the top geometry of the screen for the determination of snow volume and weight at a later stage. Since the shape of the screen is known to be affected by the wind load, a period with mild or no wind was chosen for scanning. The speed of the wind on the scanning day was 5 m/s from SE, possibly resulting in minor effects on the shape of the screen, if at all. The temperature at the time of the scanning was +7°C, and the average humidity was 97%.

The second scanning was performed in February 2013, during a period when the temperature had been for a few days just above zero, and the snow was beginning to melt. The temperature during scanning was -1°C, the average humidity was 86% and the wind speed was 2 m/s from NE. As during the first epoch, scanning was carried at the front of the screen and at the top of the screen. In February, the screen was covered by thawing snow (Figure 3). Due to the weight of the snow, remarkable displacements of the acoustic screen were expected.

During the scanning process, a cube of snow with dimensions of 13x13x14 cm was weighed by a household digital scale to assess the total weight of the snow. The weight of the cube was 0.61 kg. Since the snow volume was determined from the TLS data to be 231.3 m³, then the total weight of the snow on the acoustic screen was estimated to be 70 tons.

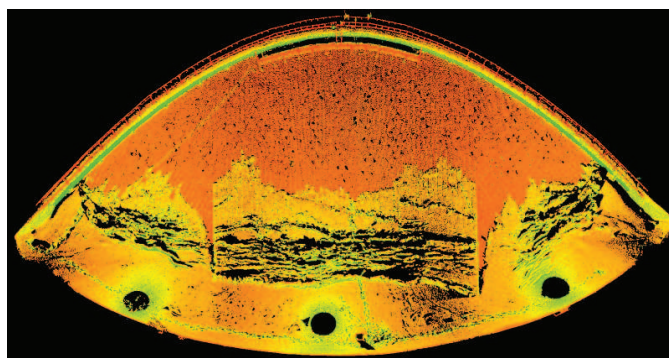


Figure 3 The point cloud of the acoustic screen, irregular shapes in the middle of the screen denote edges of snow-cover, uncoloured circles denote the locations of the scanner

The third scanning epoch took place in May 2013, at the end of the winter period. The temperature at scanning was +27°C, the average humidity was 86%, and the wind speed was 6 m/s from SW. Due to the speed of wind, the shape of the acoustic screen was probably deviating marginally from its dominating position, if at all. In May, the recovery of the structure was expected. The scanner was centred above two geodetic network monitoring points in front of the acoustic screen.

For future projects to receive more accurate and reliable georeferencing results larger than 3 inch TLS targets should be used in at distances exceeding 40 to 50 m.

5 DATA PROCESSING AND RESULTS

Laser scanning data processing was carried out in two stages, the first stage included point cloud processing using 3D Point Cloud Processing Software Leica Cyclone 8.0, where a point at the bottom of each connecting cable was identified for every epoch. Using these cable

connection points, 3D TIN (Triangular Irregular Network) surface models of each epoch were created and compared. The second stage included importing the comparison data into Autodesk AutoCAD Civil 3D 2013, where surface comparison results were analyzed.

The comparison between the November and February data show that up to 60% of the screens total area had deflected under a load of 70 tons of thawing snow. The comparison results show deflection up to -11.3 cm at the bottom of the screen (depicted by dark colours in Figure 4). The snow load on the lower part of the screen yields stronger tensile force to the front arch, causing the cables to deform. The comparison results show that 20% of the screen at the higher end near the front arch rose upwards as much as +3.1 cm (see Figure 4 the Eastern side). 20% of the screen, located at the centre, remains practically unaltered (see Figure 4 in). The determined magnitudes of the deformations were as expected.

The comparison between the November and May data shows that the shape of the screen had not regained its original geometry. 72% of the screen had in fact risen at the centre part of the screen compared to the surface in November. The results show a rise up to +12.1 cm (see Figure 4 depicted in red). Peripheral parts at the screen edges (see Figure 4) had not recovered from the snow load, indicating that 1% of the surface in May was still lower, up to -3.8 cm, than in November. Only 27% of the screen regained fully the initial shape (as in November) (see Figure 4).

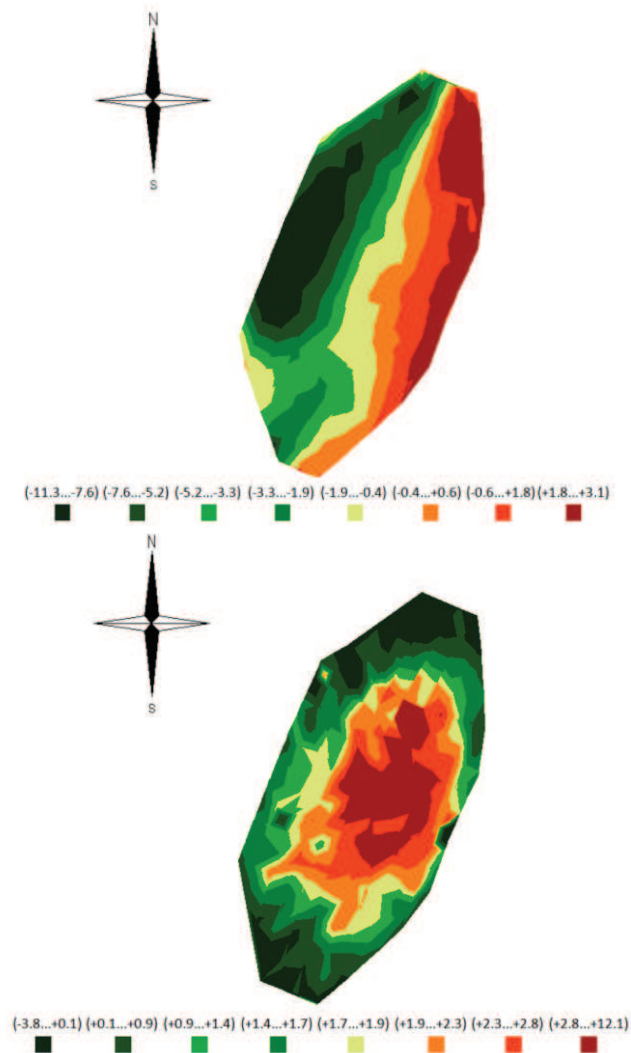


Figure 4 Results of the comparison of surfaces November and February (left); Results of comparison of surfaces November and May (right) (values in cm). Note differences in scales

6 CONCLUSIONS

In this case study, TLS data was used to determine deformations of a cable supported roof structure, a large acoustic screen at the Tallinn song festival grounds in Estonia. A geodetic monitoring network was established around the acoustic screen. The TLS survey was conducted in three epochs, in November under the construction's own weight, to determine the initial state of the screen; in February under a load of thawing snow, to determine the physical structural changes of the screen as a result of a snow load; and in May, when the recovery of the structure was expected.

Though TLS's are mainly considered suitable for using in temperatures above zero and preferably in dry weather the study has proven otherwise. Nowadays TLS instruments are capable in acquiring data in unfavourable environment conditions. All in all the novel TLS technology has proven to be beneficial for monitoring complex and otherwise inaccessible structures as the large-scale acoustic screen at Song and Dance festival grounds in Estonia.

ACKNOWLEDGEMENTS

The used TLS Leica ScanStation C-10 and the licensed 3D Point Cloud Processing Software Leica Cyclone is purchased within frames of the Estonian Research Infrastructures Roadmap object Estonian Environmental Observatory (funding source 3.2.0304.11-0395, project No. AR12019). This research is supported by the Prof. Karl Õiger scholarship and the Estonian Environmental Technology R&D Programme KESTA research project ERMAS AR12052. The conference INGEO2014 participation of the principal author is supported by the Doctoral School in Civil and Environmental Engineering of the Tallinn University of Technology. Prof. Karl Õiger from the Dept. of Structural Design of Tallinn University of Technology is thanked for consultation on structural matters.

The reviewers are thanked for their comments and suggestions on the previous version of the manuscript.

REFERENCES

- GONZÁLEZ-AGUILERA, D., GÓMEZ-LAHOZ, J., SÁNCHEZ, J. (2008). A New Approach for Structural Monitoring of Large Dams with a Three-Dimensional Laser Scanner. *Sensors*, 8(9), 5866-5883. doi:10.3390/s8095866
- GONZÁLEZ-JORGE, H., RIVEIRO, B., ARMESTO, J., ARIAS, P. (2011). Standard artifact for the geometric verification of terrestrial laser scanning systems. *Optics & Laser Technology*, 43(7), 1249-1256. doi:10.1016/j.optlastec.2011.03.018
- KULBACH, V. (2007). *Cable structures Design and static analysis*. Tallinn: Estonian Academy Publishers. 224 p.
- LICHTI, D. D. (2008). A method to test differences between additional parameter sets with a case study in terrestrial laser scanner self-calibration stability analysis. *ISPRS Journal of Photogrammetry and Remote Sensing*, 63(2), 169–180. doi:10.1016/j.isprsjprs.2007.08.001
- LICHTI, D. D., GORDON, J. S. (2004). Error Propagation in Directly Georeferenced Terrestrial Laser Scanner Point Clouds for Cultural Heritage Recording. *FIG Working Week, The Olympic Spirit of Surveying*. Athens.
http://www.fig.net/pub/athens/papers/wsa2/wsa2_6_lichti_gordon.pdf

- RIVEIROA, B., GONZÁLEZ-JORGE, H., VARELAB, M., JAUREGUIC, D. (2013). Validation of terrestrial laser scanning and photogrammetry techniques. *Measurement*, 46(1), 784–794. doi:10.1016/j.measurement.2012.09.018
- SCHOFIELD, W., BREACH, M. (2007). *Engineering Surveying, Sixth Edition*. Oxford, UK: Elsevier. 622 p.
- SOUDARISSANANE, S., LINDENBERGH, R., MENENTI, M., TEUNISSEN, P. (2011). Scanning geometry: Influencing factor on the quality of terrestrial laser scanning points. *ISPRS Journal of Photogrammetry and Remote Sensing*, 66(4), 389-399. doi:10.1016/j.isprsjprs.2011.01.005
- TSAKIRI, M. L., PFEIFER, N. (2006). Terrestrial laser scanning for deformation monitoring. *Proceedings of 12th FIG symposium on deformation measurement and 3rd IAG symposium on geodesy for geotechnical and structural engineering*. Baden. http://www.ipf.tuwien.ac.at/np/Publications/tsakiriLichtiPfeifer_FIG.pdf